Werk

Jahr: 1984
Kollektion: fid.geo
Signatur: 8 Z NAT 2148:55
Digitalisiert: Niedersächsische Staats- und Universitätsbibliothek Göttingen
Werk Id: PPN1015067948_0055
PURL: http://resolver.sub.uni-goettingen.de/purl?PPN1015067948_0055

LOG Id: LOG_0016
LOG Titel: Ground-based observations of a very intense substorm-related pulsation event
LOG Typ: article

Übergeordnetes Werk

Werk Id: PPN1015067948
PURL: http://resolver.sub.uni-goettingen.de/purl?PPN1015067948
OPAC: http://opac.sub.uni-goettingen.de/DB=1/PPN?PPN=1015067948

Contact

Niedersächsische Staats- und Universitätsbibliothek Göttingen
Georg-August-Universität Göttingen
Platz der Göttinger Sieben 1
37073 Göttingen
Germany
Email: gdz@sub.uni-goettingen.de

J Geophys (1984) 55:41–53

Journal of Geophysics

Ground-based observations of a very intense substorm-related pulsation event

H. Lühr, N. Klöcker and S. Thürey

Institut für Geophysik und Meteorologie der Technischen Universität Braunschweig, Mendelssohnstraße 3, D-3300 Braunschweig, Federal Republic of Germany

Abstract. A very intense pulsation event with characteristics of the high-latitude Pi2 type occurred in northern Scandinavia on 2 November 1982 during the evening hours. The ionospheric phenomena associated with this event have been measured by the newly installed EISCAT magnetometer cross, by the Finnish riometer chain, and by the STARE facilities. The magnetic disturbances on the ground are explained im terms of intense and narrow electrojets extended in the south-east to north-west direction and drifting with a velocity of more than 2 km/s in the south-west direction. Within the drifting reference frame the currents are nearly constant. The electrojets of the first two pulses had an intensity of about 4×10^5 A distributed over a width of about 20 km. Just before the onset, the magnetometer chain was located on the poleward side of a well-developed Harang discontinuity. The pulsations started concurrently with a substorm onset and lasted for 40 min. Mapping STARE measurements into the magnetosphere, we interpret the event as kinetic Alfvén waves generated near the boundary between differentially drifting plasma regions. From the combination of magnetometer and riometer measurements we conclude that only odd numbered reflections of the prime event have been observed.

Key words: EISCAT magnetometer cross – Harang discontinuity – Pi2 pulsation – Ionospheric currents – Alfvén waves

Introduction

Since two-dimensional ground-based magnetometer arrays and the STARE facility have provided new observational techniques, pulsation analysis in the range of Pc5 and Pi2 has been intensified recently. The studies of Allan et al. (1982; 1983), who found a new type of Pc5, have to be mentioned. The main characteristic of this type is a westward drifting ionospheric wave front elongated along magnetic meridians. Further investigations of Pi2 magnetic pulsations were carried out by Pashin et al. (1982) and by Samson and Rostoker (1983).

Detailed knowledge of the properties of pulsations in this frequency range is of special interest from the point of view of magnetospheric-ionospheric coupling. This is true especially for Pi2 pulsations. Bursts of Pi2 accompany substorm onsets and each intensification of the electrojet (Saito, 1961). Due to this one-to-one correspondence Pi2 might provide a key for the understanding of the physical processes governing the energy release during magnetospheric substorms.

The actual mechanism for the formation of the Pi2 is still far from resolved. Pashin et al. (1982) explain their observations as oscillating upward-directed field-aligned currents (FAC) at the western edge of the expanding substorm current system. Oscillations in the period range

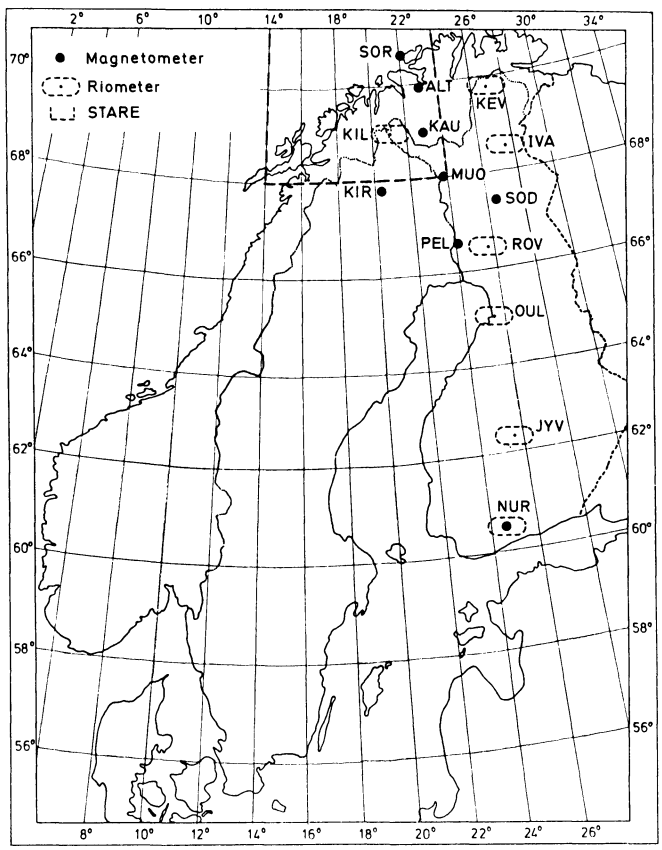

Fig. 1. Map of Scandinavia indicating the locations of the magnetometer stations (*heavy dots*), the riometer stations (*dotted ovals*), together with the STARE field of view (*dashed line*)

Offprint requests to: H. Lühr

Table 1. Coordinates of the magnetometer and riometer stations

Name	Code	Geographic coordinates		L-values	Type of instrument
Söröya	SOR	70.5°N	22.2°E	6.6	Magnetometer
Alta	ALT	69.9°N	23.0°E	6.2	Magnetometer
Kautokeino	KAU	69.0°N	23.1°E	5.8	Magnetometer
Muonio	MUO	68.0°N	23.6°E	5.4	Magnetometer
Pello	PEL	66.8°N	24.3°E	4.9	Magnetometer
Sodankylä	SOD	67.4°N	26.6°E	5.05	Magnetometer
Kiruna	KIR	67.8°N	20.4°E	5.35	Magnetometer
Kilpisjärvi	KIL	69.0°N	20.8°E	5.9	Riometer
Kevo	KEV	69.8°N	27.0°E	6.0	Riometer
Ivalo	IVA	68.6°N	27.4°E	5.5	Riomter
Rovaniemi	ROV	66.6°N	25.8°E	4.8	Riometer
Oulu	OUL	65.1°N	25.5°E	4.4	Riometer
Jyväskylä	JYV	62.4°N	25.7°E	3.7	Riomter
Nurmijärvi	NUR	60.5°N	24.7°E	3.34	Riomter + magnetometer

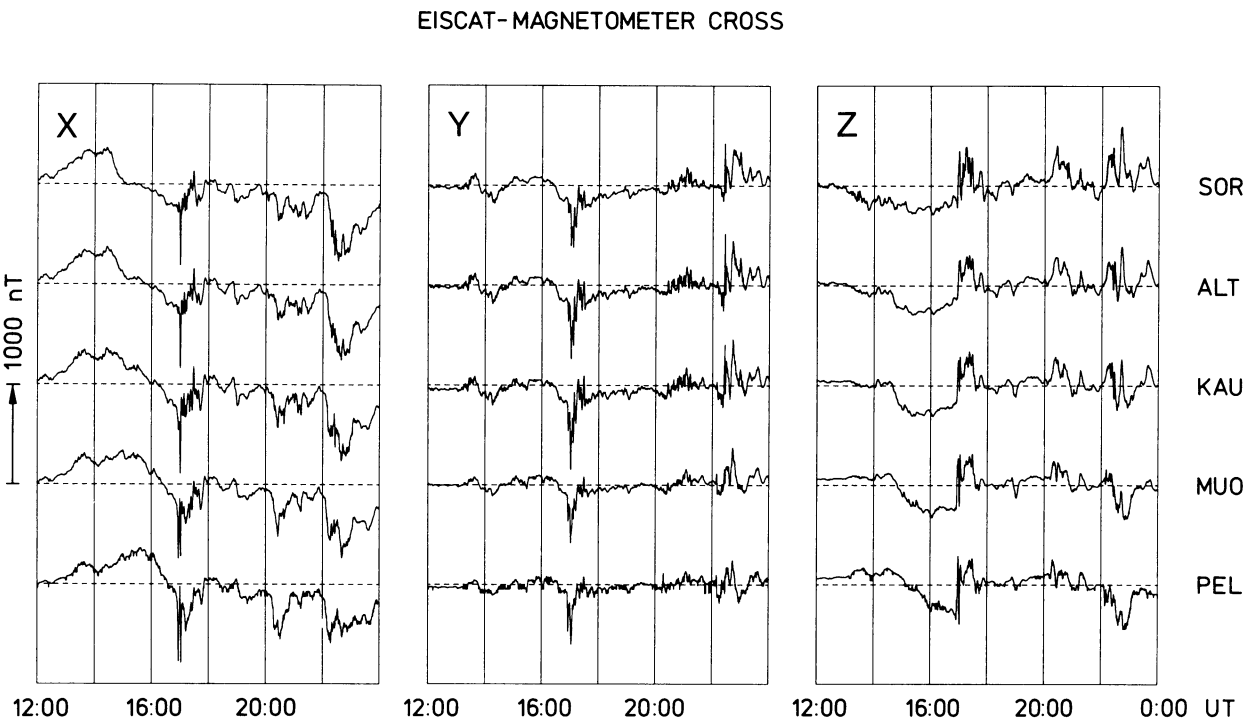

Fig. 2. Magnetic variations of the second half of 2 November 1982 along a north-south chain in Northern Scandinavia. The components *X*, *Y* and *Z* are pointing geographically north, east and downward, respectively

5–20 mHz can exist as eigen-modes of shear Alfvén waves on closed magnetic field lines (Lanzerotti and Fukunishi, 1974). The driving force of the fluctuations was assumed to be located in the equatorial plane, where the odd mode of standing waves can be excited. Samson and Rostoker (1983) regard Pi2 as the multiply reflected pulse of the initial FAC at the western end of the substorm-enhanced electrojet. Since the westward-directed electrojet expands preferentially along the Harang discontinuity, they expect the largest amplitude of the Pi2 near the equatorward border of the Harang discontinuity. An ionospheric source of Pi2 was proposed by Maltsev et al. (1974). The first impulse is generated concurrently with the brightening of the aurora. The sudden increase of electrical conductivity causes a markedly decreased electric field. This E-field transient propagates along the magnetic field lines to form a standing Alfvénic wave.

The pulsation event presented here can not be classified unambiguously. We tend to refer to it as high-latitude Pi2 pulsations as described by Samson (1982). But following the numerical classification (Saito, 1978), the observed fluctuations belong to the Pi3 type, due to their mean time period of 340 s. The nominal Pi2 band ranges from 6.7–25 mHz. However, Olson and Rostoker (1975) reported on marked peaks at 3.5 mHz in the spectra of electrojet-associated Pi2 pulsations. This is not far from the 3 mHz in our observations.

A comparison with the morphological features of the physical classes combined under Pi3 yields only a resemblance with the substorm-associated polar irregular pulsations (Pip). Among others, Pip are characterized by (Saito, 1978):

1) A period range from 100–400 s
2) An amplitude up to 100 nT

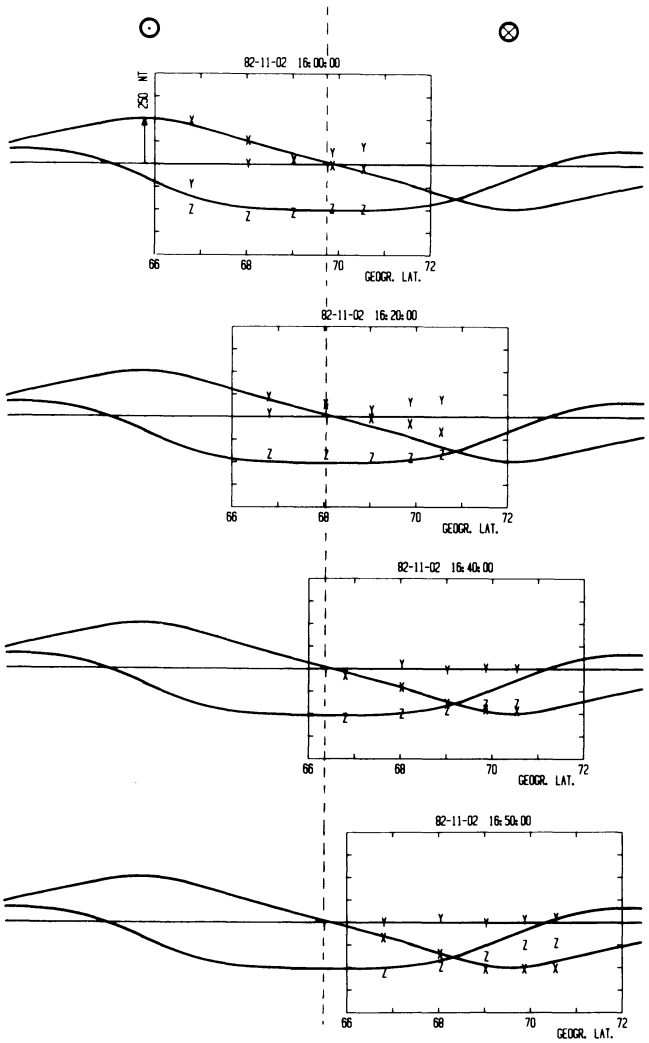

Fig. 3. Comparison of a model magnetic field (*solid lines*) of two antiparallel current bands representing the Harang discontinuity with actually measured profiles. The *crossed and dotted circles* on top symbolize the position of the centres of the westward and eastward electrojets, respectively. The *dashed vertical line* indicates the symmetry axis of the current system. The horizontal components X and Y have been rotated by 30° to minimize Y variations before being plotted into the latitude profiles

3) A duration coincident with the length of substorm there

4) Associated auroral intensity fluctuations with the approximate period range of Pip

5) A time lag between the onset of Pip at the higher latitudes and the onset at an auroral-zone station, resulting in an apparent travel velocity of 0.5–1.0 km/s towards higher latitudes

The features of the pulsations we are dealing with differ only in the direction of the travel velocity and its magnitude.

In addition to Pip, Ps6 are substorm-associated pulsations. Some of their characteristics are the following (Saito, 1978):

1) Their periods range from 5–40 min.

2) Ps6 tends to be observed dominantly in the east-west component of the magnetic field.

3) During a Ps6 event the magnetic field varies its direction concurrently with fluctuations in the direction of the ionospheric electrojet.

4) A time lag occurs from the Pi2-substorm onset to the Ps6 onset. It increases with increasing longitudinal distance between the observed point and the midnight meridian.

As regards these selected Ps6 characteristics, the morphological features of the pulsations presented here are different. The unsually large amplitude of the first two pulses of nearly 1,000 nT is much greater than the subsequent variations of the magnetic substorm. For this reason the pulsations do not seem to be a secondary effect of the polar electrojet as indicated by characteristic (3). Regarding the time period, we are now at the lower border of the nominal period range. And – the last argument against Ps6 – our event is directly correlated with mid-latitude Pi2. The onset of Ps6 should have been delayed by about 20–30 min (Saito, 1978). A clear classification of the observed event must be kept open. We tend to regard them as Pi2 like Olson and Rostoker (1975) did for Pip. It might be that the strength of the pulsations alone imply disagreements with currently observed Pi2.

Not only does the extraordinary amplitude make this event a unique one, but also the great variety of different observational systems by which it was observed. In this paper data of the new EISCAT magnetometer cross are combined with STARE and riometer measurements for a detailed description of the ionospheric properties of the event.

Instrumentation

Within this section we give a short description of the instruments from which data have been used in the present study. The location of the various instruments and facilities are shown on Fig. 1. The corresponding coordinates of measuring sites can be taken from Table 1.

Most of the magnetic data presented here are recorded with the EISCAT magnetometer cross. This project is a joint enterprise of the Finnish Meteorological Institute (FMI) in Helsinki, the Geophysical Observatory of Sodankylä and the Technical University of Braunschweig. Five of the planned seven stations were installed on a north-south chain. They have been in operation since 1 October 1982. A sixth station was run at the Geophysical Observatory Sodankylä for one year in order to determine the baseline stability. The instruments are fluxgate-type magnetometers with a measuring range of $\pm 2{,}000$ nT. The analog output signals are digitized to 12-bit words, giving a resolution of 1 nT. The data are sampled at a rate of 3.2/s and averaged, in this case, over a period of 20 s. A very stable station clock controls the measuring cycle, so that the averaging intervals start simultaneously at all stations. The bandwidth of the magnetometer is 0.5 Hz; therefore the frequency response function of the instrument is given only by the length of the averaging interval.

The digital data are stored on cartridge tapes. They have to be changed every 14 days and sent to the FMI in Helsinki. Here the data are transcribed onto a computer compatible tape. Unfortunately the binary/ASCII-converter did not work properly at PEL, so some of the data are erratic. As this malfunction produced only discrete deviations, we could correct the errors by hand for the period of interest.

In addition to the magnetic data of our six stations, minute values from the observatories Kiruna and Nurmijärvi have been used.

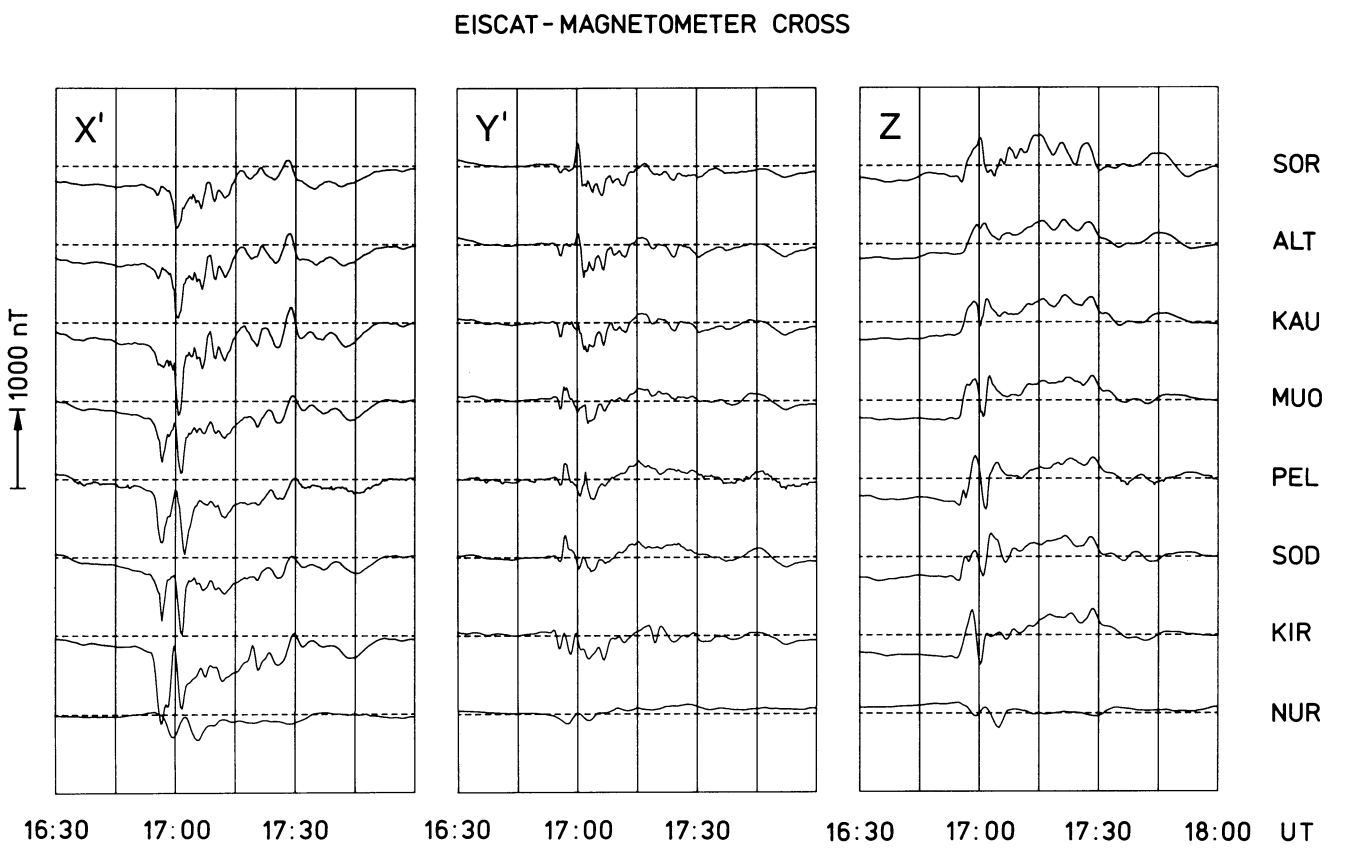

Fig. 4. Magnetic variations on an expanded time scale displaying the whole period of interest. The X- and Y-components are rotated by 35° in order to have X' pointing perpendicularly to the current flow. The stations SOD and KIR, situated at the side of the chain, and NUR in southern Finland are added. In X' a uniform dirft of the disturbances around 1700 UT can clearly be seen between SOR and PEL and, with some delay due to the long distance, down to NUR. The registration of the lateral station SOD coincides best with MUO and that of KIR best with PEL, indicating a more or less two-dimensional structure of the source

A north-south chain of eight Finnish riometers is operated by the Geophysical Observatory, Sodankylä. The ionospheric absorption measured with these instruments is recorded on a paper strip chart at a speed of 60 mm/h. These analog recordings have been digitized to 1-min values. The instrument at Sodankylä did not produce proper recordings; therefore, we could not use it for this study.

Unfortunately the sky was cloudy over all of northern Scandinavia on 2 November 1982. For this reason there are no all-sky camera recordings available.

Observations

On 2 November 1982 the magnetosphere was in a state of enhanced convection. During the afternoon hours our magnetometer chain was located beneath a relatively stable eastward flowing polar electrojet (see Fig. 2). Around 1600 UT the Harang discontinuity passed above the centre of the chain. Shortly before 1700 UT impulsive disturbances with amplitudes of up to 900 nT appeared and completely replaced the previously observed current system. During the remaining hours of this day, two more substorms occurred at around 2030 and 2230 UT.

Harang discontinuity

In this study we will pay special attention to the pulsations around 1700 UT. To do this properly it seems worthwhile to take a closer look at the preceding situation, in our case the Harang discontinuity. The parameters of the electrojets associated with the Harang discontinuity have been determined by fitting a model to the magnetic measurements. The model consists of two antiparallel sheet currents with density $j(x)=\frac{I}{\pi}\frac{b}{x^2+b^2}$. They have infinite length and are placed at an altitude of 105 km. An acceptable fit can be achieved with the following parameters:

- total current I, each: 3.7×10^5 A
- half-width of sheet ($2b$): 400 km
- distance between current centres: 800 km
- direction of jets: −60° from north

Figure 3 shows a comparison between magnetic field profiles calculated from the model (solid lines) and the actual measurements (X, Y, Z) along the N–S profile, at four different times. The horizontal components have been rotated by 30° prior to plotting, to align the Y-axis with the jets. The relative movement between the Harang discontinuity and the magnetometer chain which results from Fig. 3 can be explained by the rotation of the earth and the motion of the auroral oval in that local time sector. Consequently, the Harang discontinuity was stationary in the earth-sun system throughout the displayed period. At 1656 UT, the time of the onset of the pulsations, the centre of the westward electrojet was just overhead KAU.

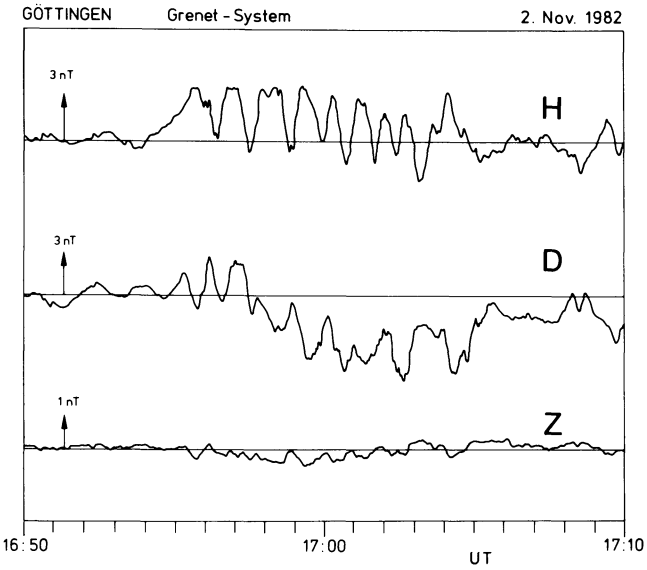

Fig. 5. Pulsation registration of a mid-latitude station. The Pi2 event at Göttingen starts simultaneously with the onset of the pulsations over Scandinavia around 1655 UT

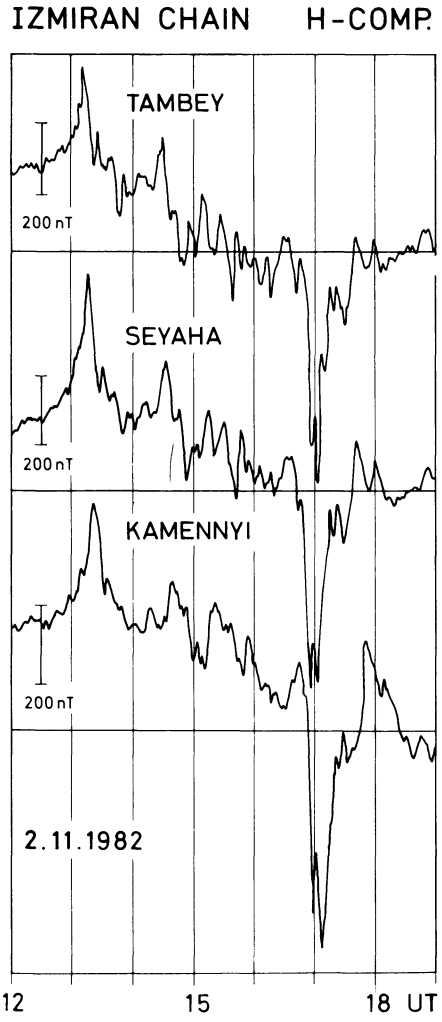

Fig. 6. Magnetic recordings from three auroral zone stations of the Izmiran Chain. The horizontal component clearly shows the signature of a substorm starting simultaneously with our pulsations. These stations are located about 50° east of our chain

Pulsation event

This long-lasting stable situation was suspended abruptly with the advent of the large pulsations. Figure 4 shows the magnetic variations around 1700 UT on an expanded time scale. In addition to our north-south chain, magnetograms from NUR, KIR and SOD are also presented. The coordinate system used for these plots is rotated by 35° about the Z-axis in order to minimize the variations in the Y'-component (see Fig. 9). On average, the horizontal disturbance vector points in the south-west direction, around $-145°$ from geographic north (compare Fig. 13). This event-oriented frame (X', Y', Z) is used in all succeeding calculations.

The onset of the pulsation event coincides with Pi2-activity at mid-latitude stations like Göttingen (Fig. 5). At auroral stations of the Izmiran chain, 49° east of our chain, we also see an onset of a substorm at 16:54 UT (about 21:50 MLT). The substorm lasted for approximately 50 min (see Fig. 6). Both observations indicate that our event is substorm-related without any delay-time, which is a general characteristic of all Pi2 pulsations. The fact that the pulsation periods, observed at Göttingen and expected at all latitudes, are not present in our magnetograms is due to the relatively low sampling rate of our magnetometer stations.

In the following we will focus on the X'-panel (Fig. 4) for a while. Despite the small extent of the magnetometer chain, the very first pulse was bounded to the southern part of the chain. The second pulse was seen, with nearly the same amplitude, by all stations (except for the more southern station NUR), but not at the same time. Consequently the disturbance drifted in the equatorward direction. This is also true for the smaller pulsations during the subsequent 40 min. The first pulse started at MUO, 1° south of the centre of the westward-directed pre-substorm electrojet. At 1656:40 UT this pulse reached its maximum amplitude (about 900 nT) at PEL. It was observed at NUR 3.5 min later. The second pulse built up over SOR at 1700 UT, at the northern end of the magnetometer chain. It arrived at NUR at 1706 UT.

We interpret the large magnetic variations as fields of drifting, but nearly constant, ionospheric sheet currents. Figures 7 and 8 show the development of the two pulses in time and space, in a sequence of four latitude profiles for each event. Both pulses look rather similar in shape and amplitude allowing a two-dimensional modelling of the field source for nearly all profiles. This assumption is supported by a comparison of the magnetograms of the stations along the chain with those of SOD and KIR, situated a distance to the east and west of the chain, respectively. SOD coincides best with MUO, and KIR best with PEL. Each pair of stations is aligned with the mean direction of the ionospheric current sheet (Fig. 9) deduced from the horizontal disturbance vector. The angle between the ionospheric source of the pulsations and the magnetometer chain is about 48°. This angle must be taken into account if we analyse the current profiles. Projected on the X'-axis, the distance of 1 latitudinal degree along the chain is reduced to 74 km.

Applying this spatial scale to Figs. 7 and 8, we can determine the width of the ionospheric current sheet from the latitude profiles. In this case we employed the line current model. In particular, we inferred a line current at a certain

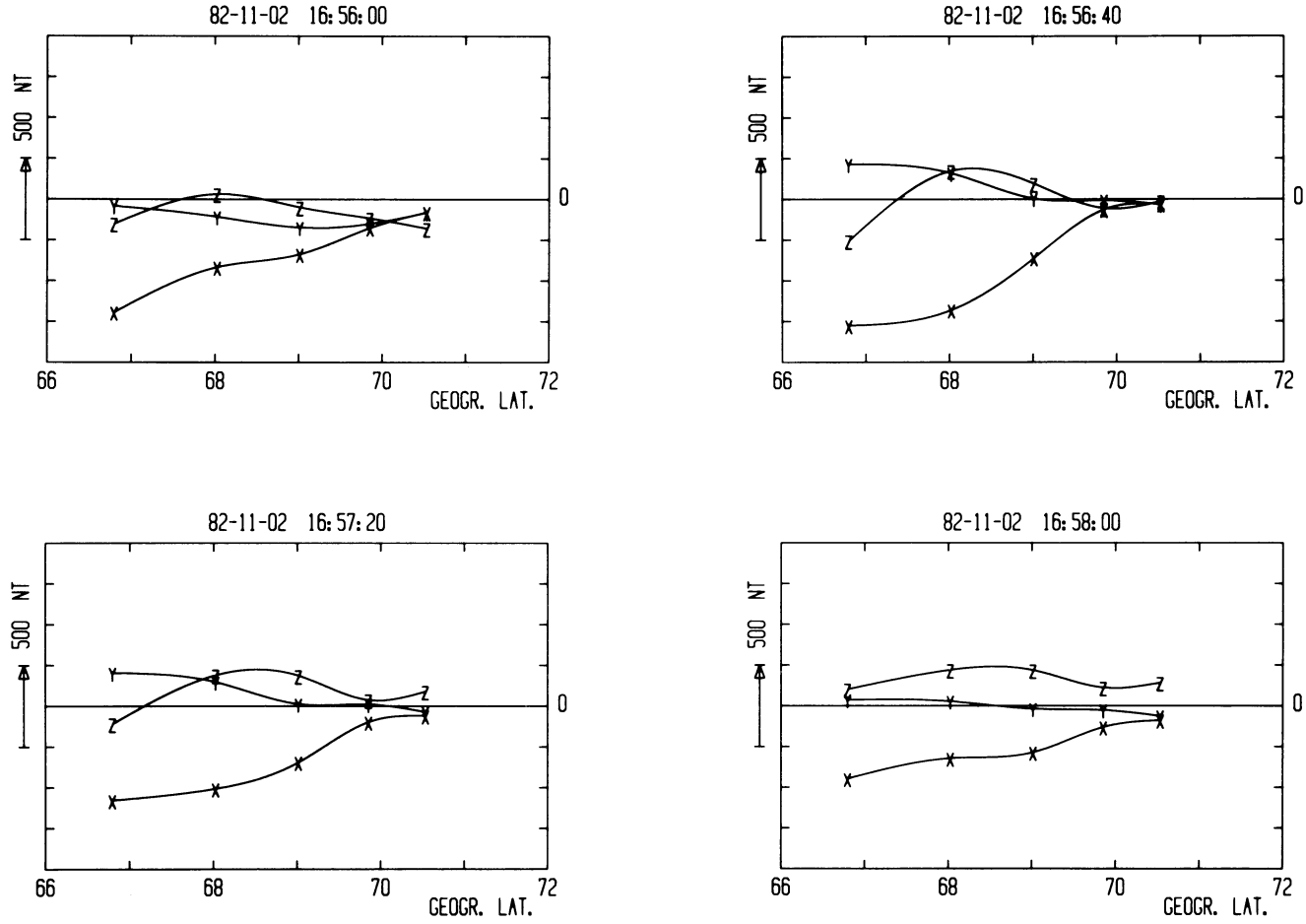

Fig. 7. Latitude profiles of the components X', Y' and Z at four selected times during the first pulse. The projected distance of one latitudinal degree equals 74 km. The disturbance grows at MUO (68° N) and moves to the south, which can best be identified by the zero crossing of Z. The profiles are computed by spline interpolation

height and an equivalent mirror current in the ground. The mirror current simulates the induction effects which have to be taken into account due to the steep slopes of the magnetic variations. Furthermore, the mirror current is symmetrical to the ionospheric current with respect to the conductopause, the upper boundary of a perfectly conducting layer called the 'conductosphere', but has an inverse direction.

We varied the model until we achieved an acceptable fit between the calculated fields and the measurements. The model configuration obtained is shown by Fig. 10a. Figure 10b contains a comparison between the model field distribution (solid lines) and the measured components in the rotated frame at 1701 UT. The estimated depth of the conductopause, of 90 km, is in good agreement with results published by Mareschal (1976).

For the conversion of the model line current to an ionospheric sheet current we used the technique proposed by Kertz (1954). He has shown that the magnetic field distribution of a line current, I, at height h_l and $x=0$ can also be generated by a sheet current with density $J(x)$ at height $h<h_l$:

$$J(x)=\frac{I}{\pi}\frac{h_l-h}{x^2+(h_l-h)^2}.$$

If we assume $h=105$ km (altitude of Hall current) and take the inferred $h_l=115$ km, we get a half-width of the sheet current of 20 km. Within the half-width, about 80% of the total current is confined. Given the measurements would be uncertain by 5%, which is a rather conservative assumption, the height h_l of the line current could vary within ± 5 km. This deviation generates an uncertainty in current width of ± 10 km.

The X'-component of KAU does not fit the model well. At this station an enhancement of the horizontal variations by about 10% can be observed in all profiles. Such behaviour has been noticed before (Jones, 1981) and might be due to an anomalous conductivity in this area.

In summary, the following parameters are deduced from the model:

– total current:	3.7×10^5 A
– width of sheet $2(h_l-h)$:	20 km
– direction of jet:	−55° from north
– depth of conductopause:	90 km

If we recall the parameters of the electrojets associated with the Harang discontinuity, we see a remarkable agreement in total current and flow direction. The width of the jet, however, is extremely narrow. The drift velocity v_d of the ionospheric currents perpendicular to their flow direction is deduced from the time differences between the minima of X' at various sites. Excluding the growth phase of the pulses, when the ionospheric source seems not to move, we get $v_d=2.2$ km/s between ALT and PEL and $v_d=2.5$ km/s

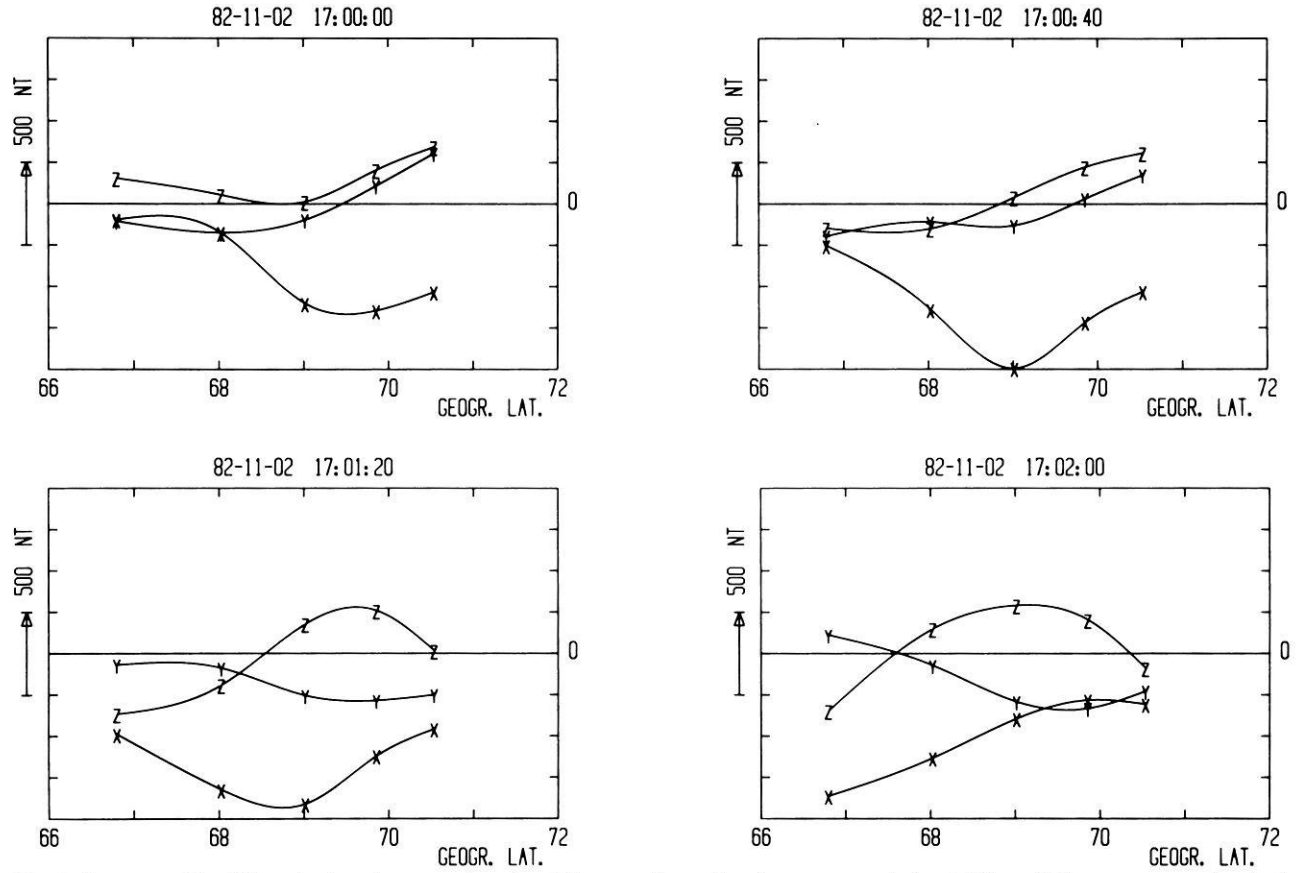

Fig. 8. Same as Fig. 7 but during the second pulse. The two-dimensional structure of the drifting field source can clearly be seen by these plots. The value of X'_{min}, a measure for the total current, is more or less the same during the whole interval. The structure drifts at 2.2 km/s in the negative X'-direction

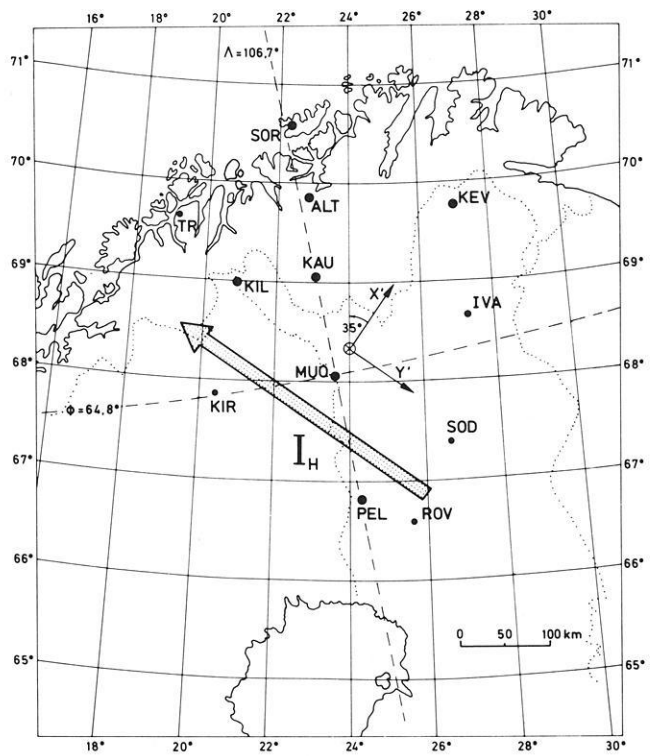

Fig. 9. Illustration of the event-oriented coordinate system and the geometry of the electrojet

between PEL and NUR. Since the time differences between distinct pulses during the 40 min are nearly the same at all stations, the whole event seems to be predominantly a wave-like phenomenon. Transformed into a coordinate system moving with v_d, the ionospheric source is stationary in time compared with the observed time period on the ground.

Comparison with riometer observations

Cosmic noise absorption measurements recorded in the auroral zone are of special interest for electrojet studies. The absorption is produced by increased ionization of the ionospheric D layer. Since the ionization of this layer is due to precipitating particles, conclusions about the location of field-aligned currents can be drawn.

Figure 11 shows stacked plots of the Finnish riometer chain. KIL, situated about 300 km west of the chain, has been included to substitute SOD. The riometer recordings look rather similar over the whole north-south extent of more than 1,000 km. At around 1700 UT the absorption increases rapidly reaching peak values beyond 6 dB. Subsequently, the absorption decreases gradually, going through a number of relative maxima.

A direct comparison with the magnetic observations is of special interest as regards the correlation between particle precipitation and individual magnetic pulses. For this purpose, riometer recordings at IVA, KIL, and ROV are com-

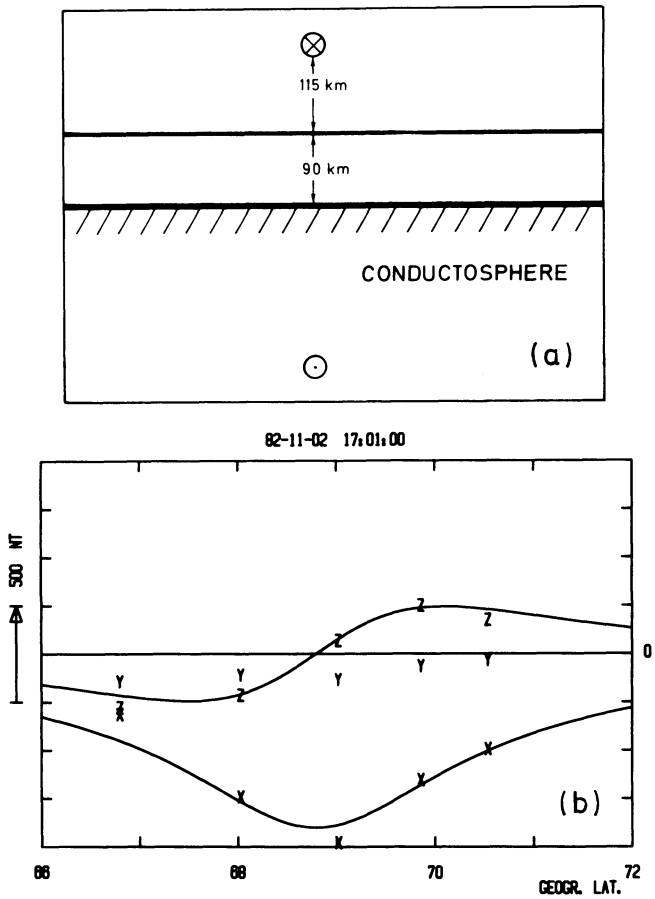

Fig. 10a and b. Comparison with a current model including induction effects. **a** The model consists of a line current at a certain height and a mirror current symmetrical, to the former, with respect to the conductopause representing the induction in the earth. **b** Best fit of the model magnetic field components (*solid lines*) to the actual readings (X', Y', Z)

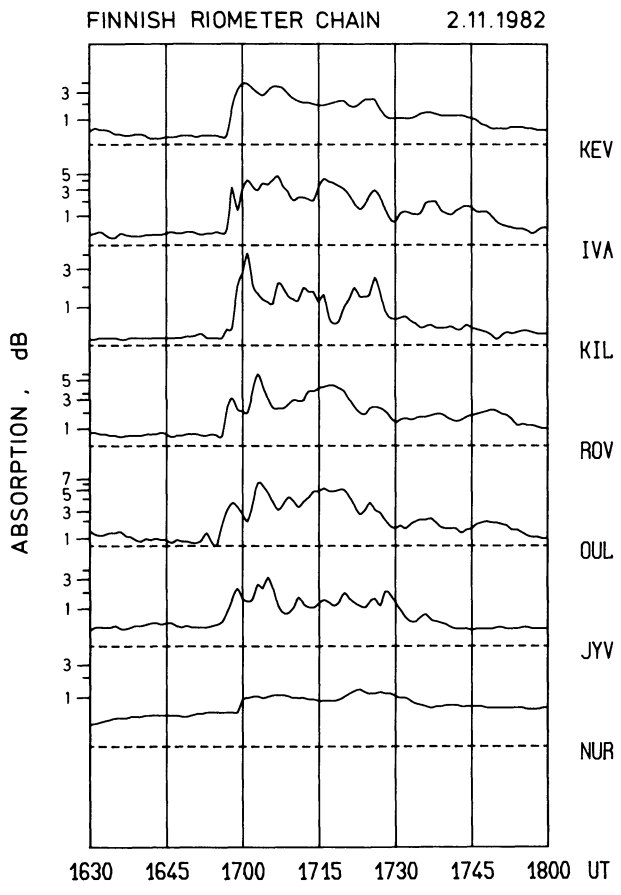

Fig. 11. Ionospheric radio noise absorption recorded by the Finnish riometer chain

bined with the X' components of ALT, KAU, and PEL, respectively, and presented in Fig. 12. In addition, the autocorrelation functions of X' are plotted in order to emphasize the periodicity of the pulsation event. We find a striking correspondence between absorption peaks in radio noise and negative deviations in X', i.e. maxima of the autocorrelation function. Furthermore, the good correspondence between distant sites underlines, again, the two-dimensional configuration of the source. The combined stations are aligned roughly with the Y'-axis (Fig. 9). Nevertheless, there are discrepancies, e.g. between the first steep increase in radio noise absorption at IVA and the first pulse at ALT, which might be due to inhomogeneities along Y'.

The correlation is best seen between KAU and KIL, which are not well aligned with the Y'-axis but relatively close together. The correlation indicates the direct relation between enhanced particle precipitation and pulsations. This is an important fact for the physical interpretation of the pulsations. The one-to-one correspondence, however, implies a further aspect, which will be discussed later. For the present, we can conclude that positive maxima in the X'-component of the magnetic field must be different from negative extrema, because only negative deviations coincide with enhanced noise absorption. This aspect may also concern the determination of the background field.

Separation of background field

The separation of the first two pulsation periods from the background field is a relatively simple task. Due to their large amplitudes, errors in the actual base line determination provide a minor effect on the interpretation. Therefore, we can be fairly sure that the first two periods were not produced by an alternating current system but by separately propagating systems with similar properties and the same direction of flow.

As already pointed out by Pashin et al. (1982), any currently used separation technique would influence the data and lead to misinterpretations. The example outlined in their publication is the effect of the pulse response function on high-pass filtered data. This leads to oscillations advancing the rapid switch-on of the currents. In addition, filtering introduces an artificially determined base line which may deviate significantly from the true one. If the base line is the output of a low-pass filter, the remaining fluctuations can be interpreted as being generated by alternating currents. Furthermore, if these currents are caused by wave reflections at the ionosphere (which will be considered in the next section), we must expect consecutive wave fronts with changing E-field directions. This would be the case if the waves travel along the ambient magnetic field bounded by the ionospheres in the two hemispheres. At each reflection the electric field changes its sign. A negative deflection in X' would be related to an odd-numbered re-

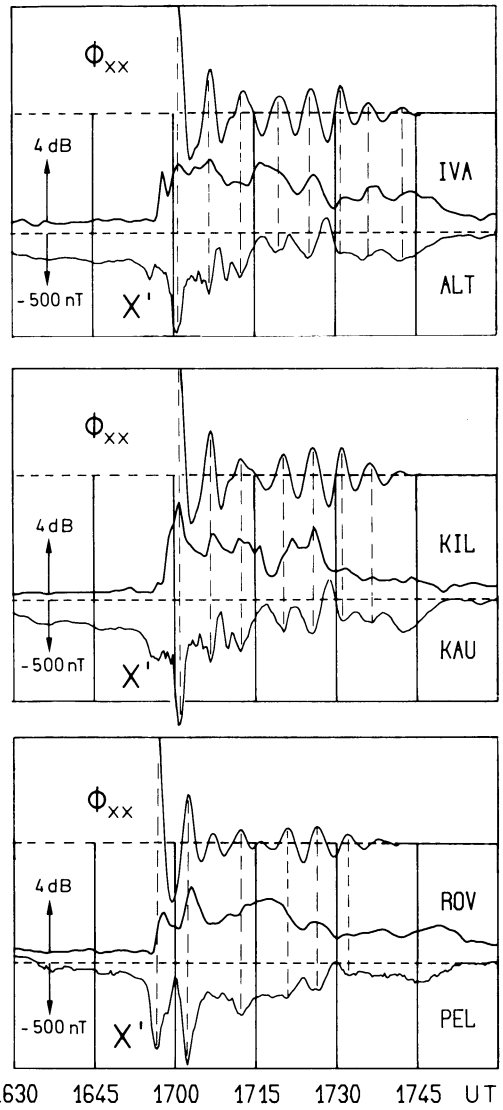

Fig. 12. Synoptical presentation of magnetometer and riometer recordings from related sites. The X'-component is displayed on the *bottom panel* and the ionospheric absorption in the *middle*. Negative deflections in X' and absorption maxima coincide best between KAU and KIL (*vertical dashed lines*). The coincidence between individual events is emphasized by adding the autocorrelation function of the magnetic registrations, displayed on the *top panel*. The autocorrelation function emphasizes the individual pulses of the event

flection of a wave and a positive to an even-numbered, respectively.

A comparison with riometer data, however, favours the interpretation that only current systems with predominantly north-west directed ionospheric current bands occurred. Otherwise the riometer data should show variations with half the period of the magnetic pulsations, because both wave types are accompanied by upward directed electric fields and precipitating particles. Thus the background magnetic field obtained by filter operation would not represent the actual conditions. These difficulties, inherently coupled with the separation techniques mostly used in Pi2 analyses, may also be relevant in their interpretation. Further analyses will be necessary.

Comparison with STARE

The drift velocity distributions of the ionospheric electrons, as seen by STARE, in conjunction with our observed horizontal magnetic disturbance vectors, are shown in Fig. 13 for selected times. At 1651:40 UT STARE displays an overall south-eastward directed drift pattern typical for the poleward side of the Harang discontinuity. At 1656:40 UT the disturbance marks a clear border between a southward electron drift on the poleward side of the STARE field of view and an eastward drift on the equatorward side. After the first pulse at 1659:00 UT the previously disturbed region is completely occupied by a uniform southward directed electron drift. Mapped into the magnetosphere, this evoluation can be interpreted as a transition from a dawnward-directed to an earthward-directed plasma convection. The first pulse is then correlated with the discontinuous border between these two regions.

The second pulse differs from the first one because it is embedded in a turbulent, but mainly equatorward directed, drift (displayed at 1700:00 UT and 1701:40 UT). During the subsequent time interval this condition does not change remarkably. A typical example is shown in the last panel of Fig. 13 (1705:00 UT). During the whole pulsation event STARE observed only south-eastward directed one-dimensional drift structures. Drift velocity vectors with westward components appear, only confined in small regions, and seem to be of turbulent character. Thus this comparison supports the conclusion drawn in the last section that the ionospheric sheet currents flowed only in one direction and did not change their sign.

Discussion

In our opinion, the observed disturbances can be explained by means of MHD theory. Changes in the magnetospheric convection electric field are transmitted by shear Alfvén waves along magnetic field lines to the ionosphere, accompanied by strong field-aligned currents and particle precipitation (Vasyliunas, 1970; Rostoker and Boström, 1976; Goertz and Boswell 1979; Lysak and Dum, 1983). The induced current system has been studied by Maltsev et al. (1977) and Mallinckrodt and Carlson (1978). Since the magnetic observations indicate a predominant two-dimensional structure of the associated currents, it is a relatively simple task to compare the observed to the theoretically deduced parameters.

We chose the coordinate system in such a way that the y-axis points horizontally along the ionospheric structure in a south-east direction. No y-dependency is considered. The z-axis is parallel to the earth's magnetic field $\mathbf{B}_o$, i.e. z points approximately vertically down, and x completes the right-hand system. In the cold plasma approximation the polarization current is continued by field-aligned currents for which the following equation holds:

$$I_z = \Sigma_W \frac{\delta E_x}{\delta x}$$

with $\Sigma_W = (\mu_0 v_A)^{-1}$, where v_A is the well known Alfvén velocity $v_A = B_0/\sqrt{\mu_0 \rho_i}$. E_x is the wave electric field which is assumed to be generated by disturbances in the convective plasma flow in the magnetosphere near the equatorial plane. Integration along x between the extrema of E_x yields the field-aligned sheet current density

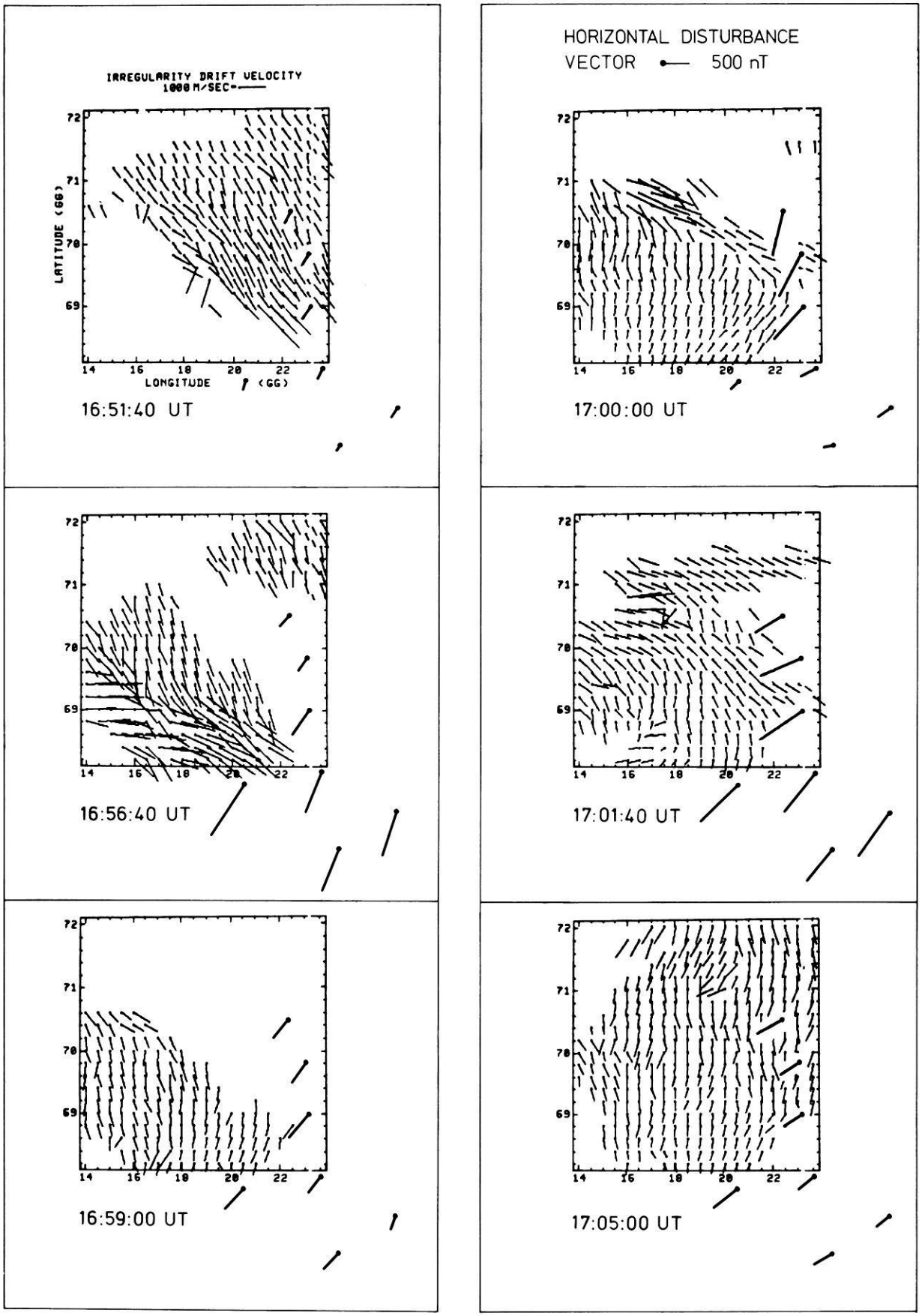

Fig. 13. Electron drift velocity from STARE and horizontal disturbance vectors of the magnetic field

$$J_z = \Sigma_W \Delta E_x. \quad (1)$$

If the perpendicular scale length of E_x becomes comparable to the ion gyroradius or electron inertial length, the properties of the Alfvén wave changes. Then the field-aligned electric field is no longer negligible, and the wave is called a kinetic Alfvén wave. Equation (1) is, however, still valid (Goertz and Boswell, 1979; Lysak and Carlson, 1981). The so-called flux tube conductivity Σ_W can be positive and negative according to the wave propagation direction along z. Its value ranges from 0.1 to 1 Ω^{-1}. Current continuity at the ionospheric boundary of the flux tube leads to the expressions

$$E_{I_0} \approx 2 \frac{|\Sigma_W|}{\Sigma_P} E_0^{\downarrow}, \quad (2)$$

$$E_0^{\uparrow} = \frac{|\Sigma_W| - \Sigma_P}{|\Sigma_W| + \Sigma_P} E_0^{\downarrow}, \quad (3)$$

$$J_{I_x} = \Sigma_P E_{I_0}, \quad (4)$$

Equation (2) is an estimation for the ionospheric electric field amplitude in x under disturbed conditions ($\Sigma_p \gg \Sigma_W$). $E_0^{\downarrow}$ is the amplitude of the wave field component E_x. Σ_p is the height-integrated Pedersen conductivity. Effects of inhomogeneous ionospheric conductivities are neglected here. They have been treated by Ellis and Southwood (1983) and Glaßmeier (1984). Equation (3) describes the amplitude of the reflected field $E_0^{\uparrow}$ in relation to that of the incoming field $E_0^{\downarrow}$. Since the ionosphere was strongly ionized during the pulsation event, almost all wave energy must have been reflected back into the magnetosphere. Therefore $E_x^{\uparrow}$ can be expected to be of the same order of magnitude as $E_x^{\downarrow}$, but has switched sign. The case $\Sigma_p \approx \Sigma_W$ is very unlikely (Southwood and Hughes, 1983) and therefore is also neglected. In this case the ionosphere would act as a perfectly matched load at the end of a field line. Then the reflection coefficient is zero. The geometry of this complex current system is illustrated in Fig. 14.

With the above equations we can estimate fields and currents of the first two extreme disturbances. The observed magnetic variations originate from the ionospheric Hall currents along the wave front. The total current was of the order of 4×10^5 A, yielding a height-integrated current density $J_{I_y} = -20$ A/m. The width of the current strip was taken to be 20 km. The STARE drift velocity vectors are not corrected and therefore preliminary. For strong ionospheric electric fields we have to take into account that the observed irregularities have a tendency to drift more slowly than the ambient electrons (Schlegel, 1983). For this reason the electric field can be assumed to be at least of the order $E_{I_x} \approx -100$ mV/m. The height-integrated Hall conductivity then comes up to $\Sigma_H \approx 200\ \Omega^{-1}$. This is a very high value but might be realistic for this special event. Marklund et al. (1982) found Hall conductivities $\Sigma_H \leqq 90\ \Omega^{-1}$ on a sounding rocket flight. Under the unusual conditions given, $\Sigma_H/\Sigma_P = 5$ is also a reasonable value (Brekke et al. 1974; Wallis and Budzinski 1981). Then we have $\Sigma_P \approx 40\ \Omega^{-1}$ and $J_{I_x} = -4$ A/m. For the oppositely directed field-aligned sheet currents at the poleward and equatorward side of the jet it follows that $|J_z| = 2$ A/m. Finally we get for the amplitude of the incident electric wave field $E_0^{\downarrow} \approx 2$ V/m, if $\Sigma_W \approx 1\ \Omega^{-1}$ is assumed. The order of magnitude of $E_0^{\downarrow}$ seems to be adequate for an extraordinary magnetospheric source, in comparison to observations reported by Mozer et al. (1980). All values are listed in Table 2.

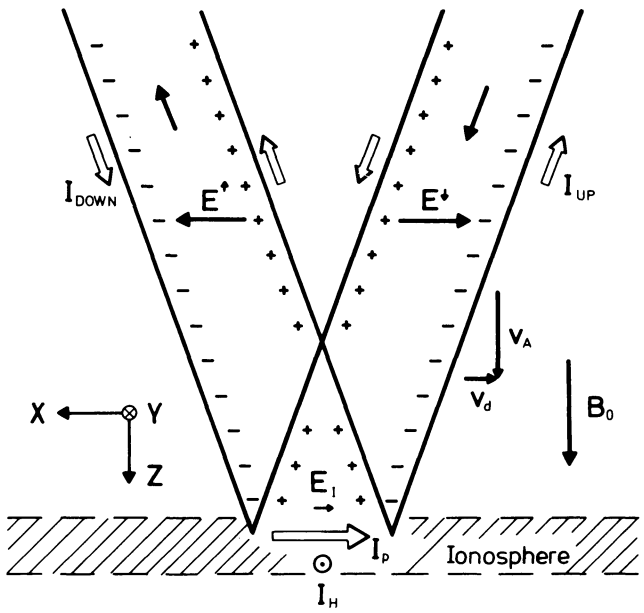

Fig. 14. Schematic cross-section of the wave front and related current system near the ionosphere. The magnetospheric source drifts relative to the ionosphere. In the drifting frame the features are time independent. In an interference region above the ionosphere the electric field of the down-coming and reflected waves nearly cancel

Table 2. Parameters of the disturbances

Observed or assumed (*)	Derived
$d = 20$ km	
$I_y = -4 \cdot 10^5$ A	$J_{I_y} = -20$ A/m
$E_{I_x} \leq -100$ mV/m	$\Sigma_H \geq 200\ \Omega^{-1}$
(*) $\Sigma_H/\Sigma_P = 5$	$\Sigma_P \geq 40\ \Omega^{-1}$
	$J_{I_x} = -4$ A/m
	$\lvert J_z \rvert = 2$ A/m
(*) $\Sigma_W = 1\ \Omega^{-1}$	$E_0^{\uparrow} = 2$ V/m

In accepting the MHD-model for the observed disturbances, further questions arise. One concerns the apparent lack of reflected waves from the opposite hemisphere. If waves are excited near the equatorial plane, we can expect them to propagate symmetrically in both hemispheres. As the parameters show, the ionosphere has to be considered as an excellent reflector on which the electric field reverses its direction. Consequently, current systems with alternating signs are expected to pass over the observer. The model suggested, e.g. by Samson and Rostoker (1983), describes Pi2 pulsations as multiply reflected waves.

As far as we can interpret our data in comparison with riometer and STARE measurements, this model does not hold for the pulsation event under discussion. The autocorrelation functions of the X'-component of all stations (Fig. 15) show a distinct repetition period of ~ 340 s indicating oscillations in a bounded system. But on the ground only odd-numbered reflections have been detected, i.e. ionospheric sheet currents flowing in a north-west direction. A possible decoupling mechanism between the magneto-

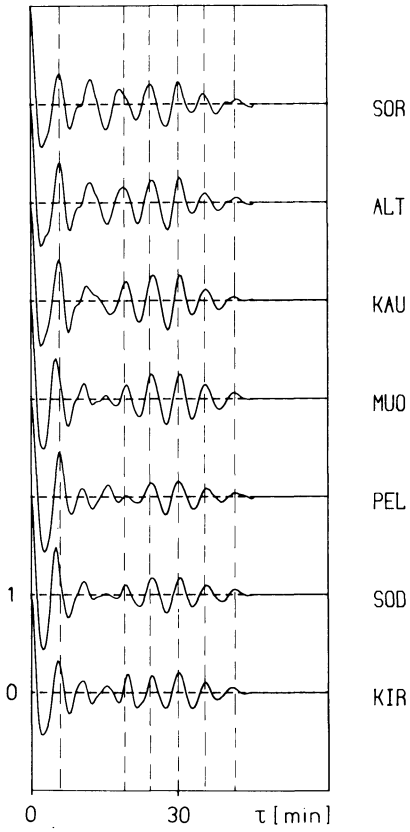

Fig. 15. Autocorrelation functions of X'. The correlated time interval contains the whole pulsation event. The mean period of 340 s can clearly be seen

sphere and the ionosphere for Alfvén waves is studied by Lysak and Dum (1983). A selective reaction of the near-earth magnetosphere on the incident wave is, however, not discussed in their model. The source region may also affect the wave, but has not been considered up to now.

Another important property of the disturbing waves is their narrow spatial extent perpendicular to the front direction. The wave length observed in the magnetic field at the ground is not identical to the spatial distribution of the ionospheric currents. The typical width of the currents is of the order of a few tens of kilometers. The fact that these waves could be observed on the ground is due to the spacing of the wave fronts. The individual wave fronts follow one after the other in a distance of more than 500 km. Thus the spatial spectrum also contains wave numbers k of the order of $10^{-5}\ \mathrm{m}^{-1} < 2\pi/h_I$, where the ionospheric height h_I is a critical value for ground observations of magnetospheric waves (Southwood and Hughes, 1983).

Waves with such a small-scale length can be regarded as kinetic Alfvén waves (Fejer and Kan, 1969, Hasegawa, 1977; Goertz and Boswell, 1979) with parallel electric fields. The existence of kinetic Alfvén waves in the near-earth magnetosphere has been established by Klöcker (1982). The parallel electric field might be strong enough to cause the observed spatially confined ionospheric ionization which occurs along with the drifting ionospheric wave fronts. In the applied model the precipitating electrons have been accelerated at the leading edge of the drifting wave front, i.e. on the equatorward side of the current system, where the field-aligned currents are upward directed (see Fig. 14).

Besides the parallel acceleration mechanism there is another effect concerning kinetic Alfvén waves. Depending on the perpendicular wave number, the phase velocity of the waves can become smaller than v_A. The dispersion relation for a cold plasma is given by

$$\frac{\omega}{k_{\parallel}} = V_A \cdot \left(1 + \frac{k_{\perp}^2 c^2}{\omega_{pe}^2}\right)^{-1/2}$$

$k_{\perp}$ and $k_{\parallel}$ are the perpendicular and parallel wave numbers relative to the undisturbed magnetic field, respectively. c is the speed of light and $\omega_{pe} = e\sqrt{n_e/\varepsilon_0 m_e}$ is the electron plasma frequency. For an understanding of the relatively long period of 340 s this effect must be taken into account.

Summary

The pulsation event discussed here belongs, in our opinion, to the Pi2 type in auroral latitudes. It is substorm correlated and seems to be generated along a plasma boundary in the magnetosphere. The specific properties of this event are the large intensity of the variations and relatively small field of the subsequent magnetic substorm. The following conclusions resulting from the discussion are:

- The magnetic perturbations originate from almost two-dimensional current systems which drift in a south-west direction with a velocity $v_d \approx 2.3$ km/s. They are observable down to latitudes $L < 3.3$.
- The mean period of the pulsations is 340 s.
- The ionospheric Hall currents are aligned to the previously existing Harang discontinuity. Their width is of the order of 20 km.
- The field-aligned currents are induced by kinetic Alfvén waves characterized by their small spatial extent perpendicular to $\mathbf{B}_0$. There is a nearly ono-to-one correspondence between the drifting wave front and the locally confined enhancement in ionization.
- Though the Alfvén waves should be multiply reflected on the ionospheres in both hemispheres, only odd-numbered reflections have been observed. This result is obtained from comparison between the untreated magnetic field recordings and other observations. Filtering would not have been an adequate technique for analysing the data.

Acknowledgements. We thank Dr. E. Kataja, Sodankylä Geophysical Observatory, Dr. C. Sucksdorff and K. Lehto, Finnish Meteorological Institute, and Mr. St. Berger, University of Tromsö for the excellent cooperation when performing our magnetic observations. We are indebted to Dr. E. Nielsen from Max-Planck-Institut für Aeronomie for interpreting STARE data and to Dr. H. and A. Ranta from Sodankylä Geophysical Observatory for providing riometer recordings. For supplying additional magnetic field data we wish to thank Mr. L. Eliasson from Kiruna Geophysical Institute, Dr. C. Sucksdorff, Helsinki, Dr. A. Zaitzev, Izmiran and Dr. H. Voelker, Göttingen.

The German part of the EISCAT-Magnetometer Cross has been funded by grants of the Deutsche Forschungsgemeinschaft.

References

Allan, W., Poulter, E.M., Nielsen, E.: STARE observations of a Pc5 pulsation with large azimuthal wave number. J. Geophys. Res. **87**, 6163–6172, 1982

Allan, W., Poulter, E.M., Glaßmeier, K.-H., Nielsen, E.: Ground

magnetometer detection of a large-m Pc5 pulsation observed with the STARE radar. J. Geophys. Res. **88**, 183–188, 1983
Brekke, A., Doupnik, J.R., Banks, P.M.: Incoherent scatter measurements of E region conductivities and currents in the auroral zone. J. Geophys. Res. **79**, 3773–3790, 1974
Ellis, P., Southwood, D.J.: Reflection of Alfvén waves by non-uniform ionospheres. Planet. Space Sci. **31**, 107–117, 1983
Fejer, J.A., Kan, J.R.: A guiding centre Vlasov equation and its application to Alfvén waves. J. Plasma Phys. **3**, 331–351, 1969
Glaßmeier, K.-H.: On the influence of ionospheres with non-uniform conductivity distribution on hydromagnetic waves, J. Geophys. **54**, 125–137, 1984
Goertz, C.K., Boswell, R.W.: Magnetosphere-ionosphere coupling. J. Geophys. Res. **84**, 7239–7246, 1979
Hasegawa, A.: Kinetic properties of Alfvén waves. Proc. Indian Acad. Sci **86A**, 151–174, 1977
Jones, A.G.: Geomagnetic induction studies in Scandinavia-II. Geomagnetic depth sounding, induction vector and coasteffect. J. Geophys. **50**, 23–36, 1981
Kertz, W.: Modelle für erdmagnetisch induzierte elektrische Ströme im Untergrund. Nachr. Akad. Wiss. Göttingen, Math.-Phys. Kl. IIa, 101–110, 1954
Klöcker, N.: Observation of guided ULF-waves correlated with auroral particle precipitation theoretically explained by negative Landau damping. J. Geophys. **51**, 119–128, 1982
Lanzerotti, L.J., Fukunishi, H.: Modes of magnetohydrodynamic waves in the magnetosphere. Rev. Geophys. Space Phys. **12**, 724–729, 1974
Lysak, R.L., Carlson, C.W.: The effect of microscopic turbulence on magnetosphere-ionosphere coupling. Geophys. Res. Lett. **8**, 269–272, 1981
Lysak, R.L., Dum, C.T.: Dynamics of magnetosphere-ionosphere coupling including turbulent transport. J. Geophys. Res. **88**, 365–380, 1983
Mallinckrodt, A.J., Carlson, C.W.: Relations between transverse electric fields and field-aligned currents. J. Geophys. Res. **83**, 1426–1432, 1978
Maltsev, Y.P., Leontyev, S.V., Lyatsky, W.B.: Pi-2 pulsations as a result of evolution of an Alfvén impulse originating in the ionosphere during a brightenning of aurora. Planet. Space Sci. **22**, 1519–1533, 1974
Maltsev, Y.P., Lyatsky, W.B., Lyatskaya, A.M.: Currents over the auroral arc. Planet. Space Sci. **25**, 53–57, 1977
Mareschal, M.: On the problem of simulating the earth's induction effects in modeling polar magnetic substorms. Rev. Geophys. Space Phys. **14**, 403–409, 1976
Marklund, G., Sandahl, I., Opgenoorth, H.: A study of the dynamics of a discrete auroral arc. Planet. Space Sci. **30**, 179–197, 1982
Mozer, F.S., Cattell, C.A., Hudson, M.K., Lysak, R.L., Temerin, M., Torbert, R.B.: Satellite measurements and theories of low altitude auroral particle acceleration. Space Sci. Rev. **27**, 155–213, 1980
Olson, J.V., Rostoker, G.: Pi2 pulsations and the auroral electrojet. Planet. Space Sci. **23**, 1129–1139, 1975
Pashin, A.B., Glaßmeier, K.H., Baumjohann, W., Raspopov, O.M., Yahnin, A.G., Opgenoorth, H.J., Pellinen, R.J.: Pi2 magnetic pulsations, auroral break-ups, and the substorm current wedge: a case study. J. Geophys. **51**, 223–233, 1982
Rostoker, G., Boström, R.: A mechanism for driving the gross Brikeland current configuration in the auroral oval. J. Geophys. Res. **81**, 235–244, 1976
Saito, T.: Oscillation of the geomagnetic field with progress of Pt-type pulsation. Sci. Rept. Tohoku Univ., 5, Geophys. **13**, 53–61, 1961
Saito, T.: Long-period irregular magnetic pulsations, Pi3. Space Sci. Rev. **21**, 427–467, 1978
Samson, J.C.: Pi2 pulsations: high latitude results. Planet. Space Sci. **30**, 1239–1247, 1982
Samson, J.C., Rostoker, G.: Polarization characteristics of Pi2 pulsations and implications for their source mechanisms: influence of the westward travelling surge. Planet. Space Sci. **31**, 435–457, 1983
Schlegel, K.: Interpretation of auroral radar experiments using a kinetic theory of the two-stream instability. Radio Sci. **18**, 108–118, 1983
Southwood, D.J., Hughes, W.J.: Theory of hydromagnetic waves in the magnetosphere. Space Sci. Rev. **35**, 301–366, 1983
Vasyliunas, V.M.: Mathematical models of magnetospheric convection and its coupling to the ionosphere. In: Particles and Fields in the Magnetosphere, B.M. McCormac ed.: pp. 60–71. D. Reidel Publishing Comp., Dordrecht, 1970
Wallis, D.D., Budzinski, E.E.: Empirical models of height integrated conductivities. J. Geophys. Res. **86**, 125–137, 1981

Received September 12, 1983; Revised February 21, 1984
Accepted March 6, 1984